RSC Chemical Biology

ROYAL SOCIETY OF CHEMISTRY

COMMUNICATION

View Article Online
View Journal



Cite this: DOI: 10.1039/d6cb00126b

Received 6th April 2026,
Accepted 30th May 2026

DOI: 10.1039/d6cb00126b

rsc.li/rsc-chembio

# Precursor gene engineering expands the loop region of the lasso peptide microcin J25

Hui-Ni Tan,[a] Julian D. Hegemann,[bc] Manuel Maestre-Reyna[ad] and John Chu *[ae]

**Microcin J25 (MccJ25) is the prototypical member of the lasso peptide family and is characterized by a mechanically interlocked structure. Scientists have long been interested in MccJ25 for its potent RNA polymerase inhibitory activity and unique threaded topology. Previous efforts to generate MccJ25 variants through precursor engineering have largely focused on amino acid substitutions – many of which were poorly tolerated by the biosynthetic machinery and resulted in diminished production. In this work, we demonstrated that the MccJ25 biosynthetic enzymes are surprisingly permissive toward insertions in the loop region. Specifically, the loop can be expanded at different positions by up to 15 additional amino acids and accommodate diverse types of amino acids. Our findings suggest that the lasso synthetase (McjC) has a sizable cavity that tolerates loop expansions. More broadly, this work establishes a new strategy for constructing mechanically interlocked molecules and potentially enables the grafting of diverse bioactive ligands onto the MccJ25 scaffold.**



## Introduction

Lasso peptides are a family of peptide natural products with diverse functions and a unique topology,[1] wherein the enzymatic maturation process likely involves a pre-folded precursor peptide, such that the tail becomes threaded through its own N-terminal macrolactam ring to form a mechanically interlocked configuration.[2–4] Microcin J25 (MccJ25) is the prototypical member of this family and the focus of the current study.[5] Its biosynthetic gene cluster encodes four genes (*mcjA* – *D*) (Fig. 1a). McjB and McjC likely form a complex that pre-folds the precursor peptide (McjA), and then catalyzes the formation of a macrolactam that encircle its own tail.[6] The mature MccJ25 binds within and obstruct the secondary channel of the bacterial RNA polymerase to inhibit transcription.[7] The membrane transporter McjD is responsible for pumping MccJ25 out of the cell to confer self-immunity.[8]

Although the mechanism by which MccJ25 inhibits transcription is well established, the molecular details of MccJ25 biosynthesis – and that of lasso peptide biosynthesis in

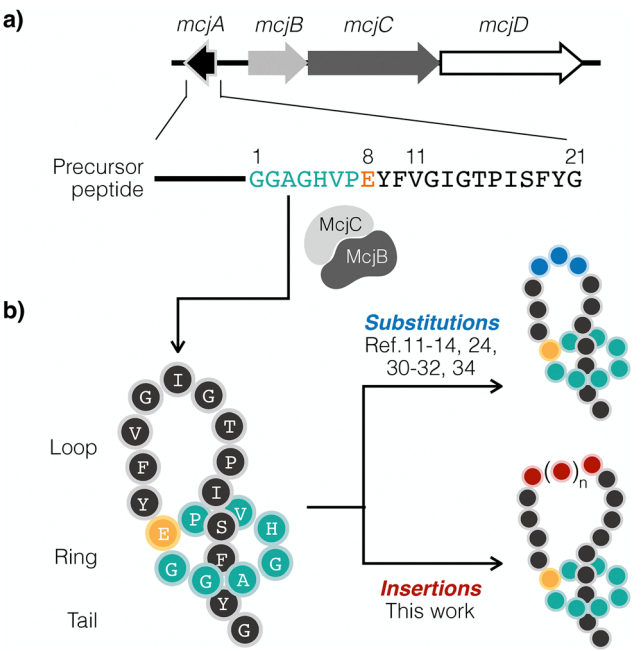


Fig. 1 (a) The biosynthetic gene cluster of MccJ25 encodes four genes, *mcjA* – *D*. The core segment within the precursor peptide (McjA), which contains 21 AAs, is processed by the biosynthetic enzymes McjB and McjC into the mature final product with the lasso topology. (b) Previous lasso peptide engineering studies have largely focused on AA *substitutions*. In this study, we report that the MccJ25 biosynthetic machinery tolerates AAs *insertions* into the loop region. Multiple AAs, including AAs that are acidic and basic, as well as large and small, can be inserted.

[a] *Department of Chemistry, National Taiwan University, Taipei 106319, Taiwan. E-mail: johnchu@ntu.edu.tw*
[b] *Institute of Pharmaceutical Biology, Technische Universität Braunschweig, Braunschweig, Germany*
[c] *Center of Pharmaceutical Engineering (PVZ), Technische Universität Braunschweig, Braunschweig, Germany*
[d] *Institute of Biological Chemistry, Academia Sinica, Taipei 115024, Taiwan*
[e] *Center for Emerging Material and Advanced Devices, National Taiwan University, Taipei 106319, Taiwan*

general – remain poorly understood. In fact, much of our current understanding of MccJ25 biosynthesis has come from precursor engineering.[9–12] For example, Severinov and coworkers replaced all core peptide residues in McjA, one at a time, with every other canonical amino acid (AA) residue. They studied the expression, maturation, export, and stability of these 381 variants.[11] McjB and McjC were able to convert 64% of these variants into mature products with the lasso topology. Subsequent studies further showed that these two biosynthetic enzymes can tolerate the incorporation of multiple non-canonical AAs in the precursor and still convert it into the lasso topology.[13,14]

In general, a lasso peptide, including MccJ25, can be divided into the loop, ring, and tail regions (Fig. 1b). Structure predictions by AlphaFold suggest that McjC contains a deep and narrow cavity that accommodates the precursor peptide during biosynthesis.[15] In this model, the ring region makes multiple contacts with the enzyme, whereas the loop region extends into the cavity and engages in comparatively fewer interactions. This model also suggests that residues within or near the ring region are less tolerant of changes, while the loop region is subject to fewer constraints and may be more readily modified.

Previous reports on engineering the precursor peptide McjA have focused primarily on amino acid *substitutions*, whereas the feasibility of *insertions* has remained underexplored. The only literature precedent entails the insertion of a single residue in the ring or the tail region.[12] Specifically, Rebuffat and co-workers reported that ring variants containing an additional Ala inserted after Gly4 or His5 were not produced in the lasso form, but instead as branched-cyclic peptides. In contrast, tail variants containing an additional residue (Gly or Asp) after the C-terminus were compatible with the biosynthetic enzymes (McjB and McjC) and produced as lasso peptides. Herein, we systematically explored AA *insertions* as a means for lasso peptide engineering and discovered that the loop region can be expanded by inserting multiple AAs of diverse types.

## Results

We began by examining whether the MccJ25 biosynthetic enzyme complex is compatible with insertions at various structural regions. All insertions were introduced by manipulating the precursor gene *mcjA via* established cloning methods. Throughout this manuscript, $^{Z}\mathbf{X}_{n}$ denotes insertion in the **Z** region of MccJ25 wherein superscript **R**, **L**, and **T** refer to having additional AA(s) in the ring, loop, and tail regions, respectively. The type and number of inserted AA(s) are specified using the standard one-letter abbreviation (**X**) and the subscript (***n***), respectively. For example, $^{L}\mathbf{A}_{3}$ indicates inserting three Ala residues in the loop region.

First, variants with a single Ala inserted into the ring and loop region in between Gly2/Ala3 and Gly12/Ile13, respectively, were generated. In addition, a variant with a single Gly placed after Gly21 for tail extension was generated (Fig. 2a and Table 1).

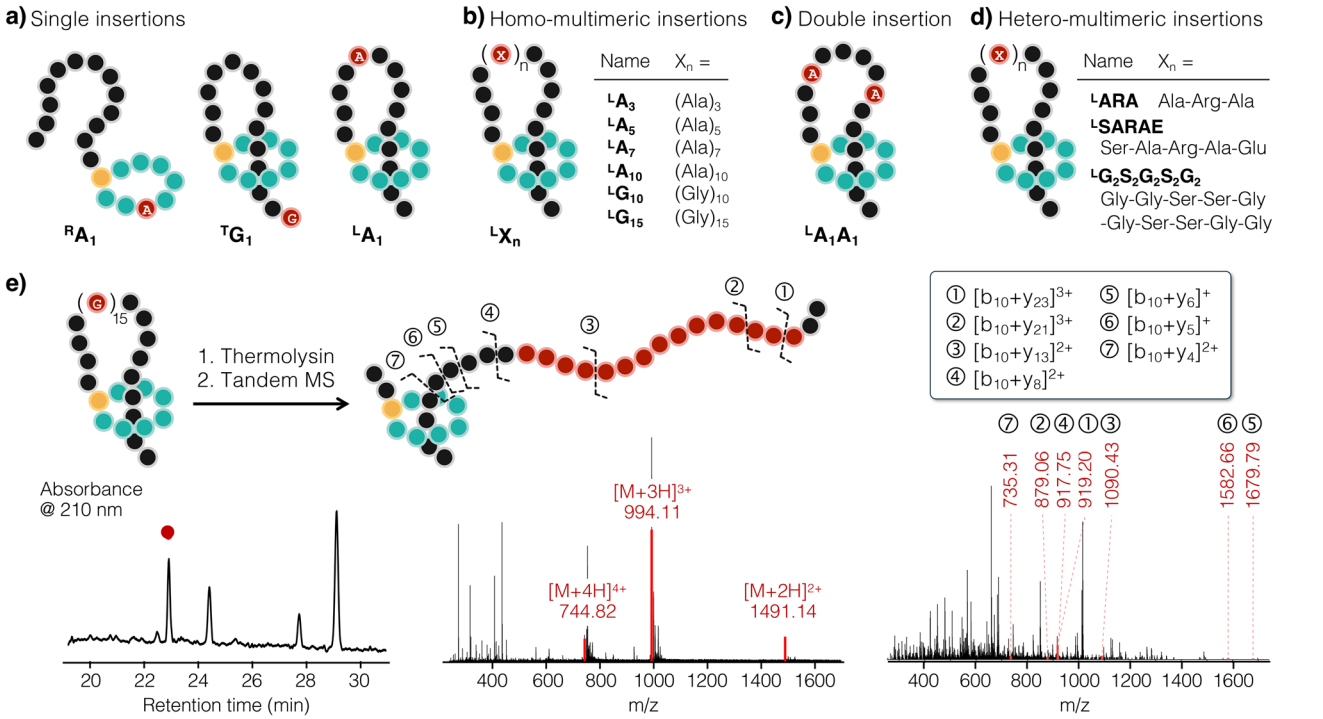


Fig. 2 The MccJ25 biosynthetic machinery tolerates a wide range of AA insertions. We systematically tested (a) single AA insertions, (b) homo-multimeric insertions, (c) double insertions, and (d) hetero-multimeric insertions. (e) Data for the $^{L}\mathbf{G}_{15}$ variant is shown here to illustrate the workflow used to confirm lasso topology. Briefly, thermolysin digestion converts the lasso peptide into a linear peptide trapped within the ring. This mechanically interlocked architecture appears as a single molecular species in MS (center), which is subjected to tandem MS for further validation (right). The lasso topology (or the lack thereof) of all variants were confirmed by this workflow; the full dataset can be found in the SI (Fig. S2–S14).

The ring insertion construct $^{R}A_1$ appeared to be a branched-cyclic peptide. On the other hand, the tail insertion construct $^{T}G_1$ was produced in the lasso form, albeit with a yield that is approximately 30-fold lower than that of wild-type (WT) MccJ25 (1 *vs.* 30 mg per liter of culture). These observations recapitulated previous reports and suggest that the biosynthetic enzymes are sensitive to insertions in the ring and tail regions.[12] In contrast, the unprecedented loop insertion construct $^{L}A_1$, wherein an additional Ala was placed in between Gly12/Ile13, was not only produced in the lasso form but also in ample amounts (32 mg $L^{-1}$). In fact, the yield was ~3% higher than that of WT MccJ25. Note that all loop constructs reported herein, unless mentioned otherwise, contained insertions in between Gly12/Ile13.

We decided to focus on insertions in the loop region of MccJ25 (Table 1). No further ring engineering was attempted, as the $^{R}A_1$ variant failed to form the lasso topology. Tail engineering was not pursued further either, as these variants are technically an *extension* rather than a true insertion. To evaluate the effects of introducing multiple additional residues into the loop region, we generated the $^{L}A_3$, $^{L}A_5$, $^{L}A_7$, $^{L}A_{10}$, and $^{L}G_{10}$ constructs (Fig. 2b). Furthermore, simultaneous insertions on both sides of the loop yielded the $^{L}A_1A_1$ construct, wherein one Ala residue was introduced in between Val11/Gly12 and another in between Pro16/Ile17 (Fig. 2c). Our largest construct adds a total of 15 residues ($^{L}G_{15}$) into the loop region, corresponding to 45 additional bonds with an estimated length of ~55 Å when fully extended.

The feasibility of inserting different types of AAs was then assessed (Fig. 2d). Three more MccJ25 variants were generated, $^{L}$**ARA**, $^{L}$**SARAE**, and $^{L}G_2S_2G_2S_2G_2$, which have insertions in the loop region with three, five, and ten additional AAs, respectively (Table 1). Ser contains a side-chain hydroxyl group that may serve as either a hydrogen bond donor or acceptor. At neutral pH, Glu has a negatively charged side-chain carboxylate, whereas Arg has a positively charged side-chain guanidinium. Arg is also the largest among the 20 canonical AAs. Proteolysis coupled to MS confirmed that all of these variants adopt the lasso topology (Fig. 2e).

We used proteolysis coupled to mass spectrometry (MS) for structural analysis, which is an established method for characterizing the composition and topology of lasso peptides (Fig. 3). Specifically, thermolysin is a protease known to cleave within the loop region of WT MccJ25 (and its variants as well), converting a lasso peptide into a linear peptide trapped within the macrolactam ring.[16] This mechanically interlocked architecture appears as a single molecular species in MS. In contrast, cleavage of a branched-cyclic peptide by thermolysin would generate two separate entities. These distinct outcomes are readily distinguished by MS. All constructs were produced in sufficient quantities for structure characterization (SI Fig. S1 to S14). The lasso peptide production yield displayed no obvious correlation between the size and sequence of the inserts (1.0 to 32 mg $L^{-1}$, Table 1). As a benchmark, we routinely obtained ~30 mg $L^{-1}$ of MccJ25, and most insertion variants have comparable yields relative to the WT. Some can even be produced at higher quantities.

The bioactivity of these MccJ25 variants was evaluated using a semi-quantitative growth inhibition zone assay. In this assay, a drop of each of the variants was added onto a lawn of *Escherichia coli* MG1655. The size of the zone (or the lack thereof) was recorded after overnight incubation at 37 °C and compared to that of the WT MccJ25 (Table 1). The $^{R}A_1$ variant was not tested (entry 2), as it was not even produced as a lasso peptide. The $^{T}G_1$ variant exhibited antibacterial activity weaker than the WT MccJ25 (entry 3), which was in line with previous literature reports. In fact, structural information obtained by X-ray crystallography showed that the MccJ25 C-terminal carboxylate mediates its interaction with the *E. coli* RNA polymerase,[17] and chemical modifications at this position were also known to compromise its antibacterial activity.[18] As for the loop variants,

Table 1 Summary of MccJ25 constructs reported herein

| Entry | Name[a] | Amino acids | Topology[b] | *m/z* calcd (obsd) | Yield[c] (mg $L^{-1}$ ± SD) | Inhibition zone[d] |
|---|---|---|---|---|---|---|
| 1 | MccJ25 | 21 | Lasso | $[M + Na]^+$ 2129.0108 (2129.103) | 31 ± 4.3 | 100% |
| 2 | $^{R}A_1$ | 22 | B/C | $[M + H]^+$ 2178.0661 (2178.116) | 1.7 ± 0.53 | n.d. |
| 3 | $^{T}G_1$ | 22 | Lasso[e] | $[M + Na]^+$ 2186.0323 (2186.833) | 1.0 ± 0.42 | 55% |
| 4 | $^{L}A_1$ | 22 | Lasso | $[M + Na]^+$ 2200.5718 (2200.379) | 32 ± 2.8 | 54% |
| 5 | $^{L}A_3$ | 24 | Lasso | $[M + Na]^+$ 2342.1222 (2342.916) | 26 ± 17 | 31% |
| 6 | $^{L}A_5$ | 26 | Lasso | $[M + Na]^+$ 2484.1964 (2484.254) | 25 ± 1.3 | 8% |
| 7 | $^{L}A_7$ | 28 | Lasso | $[M + Na]^+$ 2626.2707 (2626.289) | 12 ± 6.8 | 2% |
| 8 | $^{L}A_{10}$ | 31 | Lasso | $[M + Na]^+$ 2839.3820 (2839.305) | 9.7 ± 1.3 | 9% |
| 9 | $^{L}G_{10}$ | 31 | Lasso | $[M + Na]^+$ 2699.2255 (2699.854) | 16 ± 4.0 | 44% |
| 10 | $^{L}G_{15}$ | 36 | Lasso | $[M + Na]^+$ 2984.3328 (2984.305) | 1.0 ± 0.13 | — |
| 11 | $^{L}A_1A_1$ | 23 | Lasso | $[M + Na]^+$ 2271.0851 (2271.155) | 21 ± 2.4 | 46% |
| 12 | $^{L}$**ARA** | 24 | Lasso | $[M + Na]^+$ 2405.2043 (2405.550) | 20 ± 6.6 | 25% |
| 13 | $^{L}$**SARAE** | 26 | Lasso | $[M + H]^+$ 2621.2789 (2621.930) | 14 ± 4.8 | 20% |
| 14 | $^{L}G_2S_2G_2S_2G_2$ | 31 | Lasso | $[M + Na]^+$ 2819.2678 (2819.724) | 12 ± 1.9 | 24% |

[a] Insertions in the ring, loop, and tail regions were between residues Gly2/Ala3, Gly12/Ile13, and after Gly21 of MccJ25, respectively. The only exception was $^{L}A_1A_1$ (entry 11), in which one Ala residue each was inserted in between Val11/Gly12 and Pro16/Ile17. [b] Topology was characterized by proteolysis coupled to MS; B/C denotes branched-cyclic. [c] Yields were determined based on HPLC peak integration using a fixed amount of caffeine (0.25 mM) as an internal standard. [d] Antimicrobial activities were evaluated against *Escherichia coli* MG1655 and scored relative to that of WT MccJ25 (see SI). Antibacterial activity of the $^{R}A_1$ variant was not determined since it did not even adopt the lasso topology (n.d.). [e] Rebuffat and coworkers confirmed the lasso topology of $^{T}G_1$.[12]

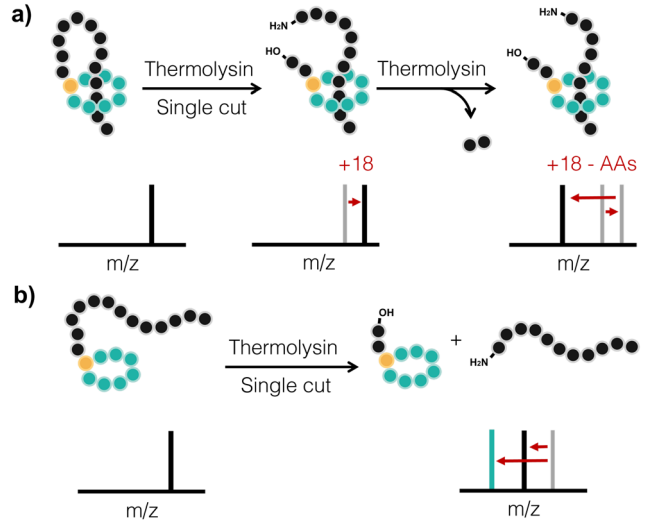


Fig. 3 Structure determination through thermolysin digestion coupled to MS analysis. (a) Digesting a MccJ25 derivative with the lasso topology generates a [2]rotaxane consisting of an axle trapped within a ring, which is detected by MS as a single entity with the net addition of one water molecule. Subsequent protease digestion may progressively remove more residues from the threaded axle, and the resulting fragments can be readily detected by MS. (b) In contrast, digesting a branched-cyclic MccJ25 derivative generates to separate fragments, both of which can be detected by MS.

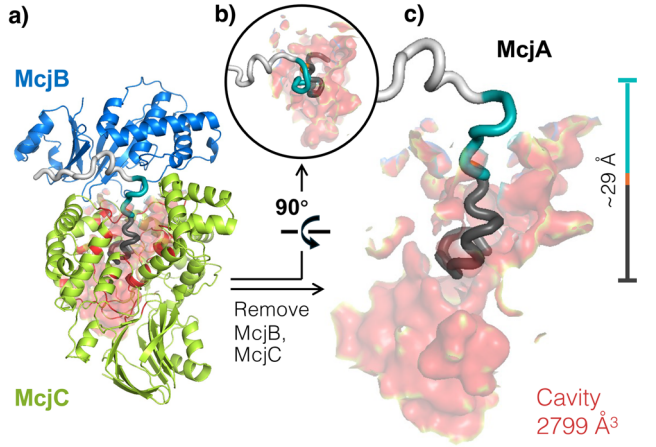


Fig. 4 (a) AlphaFold predicts that the precursor peptide McjA forms a ternary complex with the biosynthetic enzymes McjB (blue) and McjC (green). High ipTM and pTM scores (0.82 and 0.87, respectively) suggest that these predicted structures are fairly reliable. The cavity within McjC is shown in red. (b) and (c) McjB and McjC are removed to more clearly show McjA and the cavity. The peptide segment in McjA that eventually becomes the ring is shown in turquoise, and the loop and tail segments are shown in black. The key Glu8 residue, whose side-chain carboxylate condenses with the N-terminus of Gly1 to form an isopeptide for ring construction, is shown in orange. CASTpFold estimates that the cavity is ~2800 Å$^3$.

our data suggest that insertions in general weaken their antibacterial activities; however, there is no obvious correlation between the size and sequence of the inserted AAs (entries 4–14). Variants with more Ala insertions were either barely active (entries 6–8) or completely inactive (–). Interestingly, two of the largest insertion variants ($^{L}\mathbf{G_{10}}$ and $^{L}\mathbf{G_2S_2G_2S_2G_2}$, entry 9 and 14, respectively), were moderately active.

## Conclusion and discussion

In this study, we demonstrated that the MccJ25 biosynthetic enzymes can convert genetically engineered precursor variants with loop regions substantially larger than that of the WT into the lasso topology. Up to 15 additional residues can be introduced between Gly12/Ile13, and a variant containing insertions on both sides of the loop was also successfully produced in the lasso topology. Moreover, the biosynthetic enzymes appeared to tolerate insertions spanning a broad range of AA identities and sequences, including residues that are acidic, basic, large, and small. Notably, most variants were produced in yields comparable to that of WT MccJ25.

It was hypothesized that McjB and McjC form an enzyme complex that catalyzes macrolactam ring formation while folding the precursor peptide (McjA) into a thermodynamically unfavorable conformation.[15,19] Molecular dynamics simulation suggested that the pre-folded conformation is entropically disfavored and that enzymes must have played a critical role in this process.[20–22] Structural models based on AlphaFold predictions suggested that the region destined to become the loop of MccJ25 is positioned within the cavity of McjC. This rather spacious cavity is estimated to be ~2800 Å$^3$ and may be the reason behind its surprising tolerance to loop insertions (Fig. 4).[23,24] Moreover, using fusilassin as a model system, Mitchell and coworkers demonstrated that certain AA substitutions within the lasso synthetase cavity allowed the engineered enzyme to accept modified precursor peptides rejected by the WT enzyme.[24] The successful production of our insertion variants suggests that McjC can accommodate at least 15 additional residues, and potentially even more. The loop region of all of our variants adopts a compact β-turn-like shape based on the prediction algorithm designed specifically for lasso peptides (LassoPred, Fig. S15).[25,26]

Although the biosynthesis of MccJ25 tolerates a wide range of loop insertions, its antibacterial activity is much more sensitive and compromised to some extent when more than one additional residue was introduced. The primary goal of this study, however, was not to generate antibacterial MccJ25 variants *per se*, but rather to develop a more broadly applicable strategy for MccJ25 engineering. Previous studies have shown that the ring and loop regions play a critical role in recognition by FhuA, an outer membrane protein that mediates MccJ25 import.[27–30] In contrast, the ring and tail regions of MccJ25 are responsible for key interactions with RNA polymerase and is essential for its transcription inhibitory function.[17] The fact that our MccJ25 variants exhibit only moderate to no antibacterial activity is likely attributable to impaired uptake rather than diminished target engagement.

MccJ25 is a rigid scaffold that is resistant to most proteases and stable under extreme pH and temperature.[16] Nature has taken advantage of these desirable features and evolved lasso

peptides into the binder of a variety of proteins, including RNA polymerase, glucagon receptor, atrial natriuretic factor, *etc.*[1] Likewise, scientists have engineered this scaffold by grafting serial AA substitutions. For example, Marahiel and coworkers grafted the integrin binding RGD motif into MccJ25 *via* consecutive AA substitutions in the loop region.[31,32] Burk and coworkers expanded upon this strategy and reported selective $\alpha_v\beta_6$ and $\alpha_v\beta_8$ integrin binders by introducing up to nine AA substitutions throughout MccJ25.[33] Link and coworkers built two von Willebrand factor binding motifs into MccJ25 *via* AA substitutions, and the resulting derivatives showed inhibitory activity in the low micromolar range.[34] However, these constructs are generally produced in lower yields than the WT MccJ25, which underscores a major limitation in epitope grafting *via* AA substitutions. In contrast, our discovery that MccJ25 biosynthesis is compatible with tail insertion and highly tolerant to loop insertions circumvents this constraint. Tail insertion makes it possible to explore applications that require immobilization on a solid support and various display systems (phage, bacteria, or yeast).[35–38] Loop insertion tolerance hint at the potential of grafting larger and more diverse epitopes onto the MccJ25 scaffold, thereby expanding its utility for a broad range of biomedical applications.

## Conflicts of interest

There are no conflicts to declare.

## Data availability

The data supporting this article have been included as part of the supplementary information (SI). Supplementary information is available. See DOI: https://doi.org/10.1039/d6cb00126b.

## Acknowledgements

We thank the mass spectrometry research services of the Consortia of Key Technologies at National Taiwan University for technical support. This work was supported by grants from the National Science and Technology Council, Taiwan (NSTC 112-2113-M-002-005, NSTC 112-2923-M-002-005-MY3, and NSTC 114-2628-M-002-010-MY4) and the Deutsche Forschungs-gemeinschaft (DFG, German Research Foundation, project no. 528244377).

## References

1 J. D. Hegemann, M. Zimmermann, X. Xie and M. A. Marahiel, Lasso peptides: an intriguing class of bacterial natural products, *Acc. Chem. Res.*, 2015, **48**, 1909–1919.
2 M. J. Bayro, J. Mukhopadhyay, G. V. Swapna, J. Y. Huang, L. C. Ma, E. Sineva, P. E. Dawson, G. T. Montelione and R. H. Ebright, Structure of antibacterial peptide microcin J25: a 21-residue lariat protoknot, *J. Am. Chem. Soc.*, 2003, **125**, 12382–12383.
3 K. J. Rosengren, R. J. Clark, N. L. Daly, U. Goransson, A. Jones and D. J. Craik, Microcin J25 has a threaded sidechain-to-backbone ring structure and not a head-to-tail cyclized backbone, *J. Am. Chem. Soc.*, 2003, **125**, 12464–12474.
4 K. A. Wilson, M. Kalkum, J. Ottesen, J. Yuzenkova, B. T. Chait, R. Landick, T. Muir, K. Severinov and S. A. Darst, Structure of microcin J25, a peptide inhibitor of bacterial RNA polymerase, is a lassoed tail, *J. Am. Chem. Soc.*, 2003, **125**, 12475–12483.
5 F. Baquero, K. Beis, D. J. Craik, Y. Li, A. J. Link, S. Rebuffat, R. Salomon, K. Severinov, S. Zirah and J. D. Hegemann, The pearl jubilee of microcin J25: Thirty years of research on an exceptional lasso peptide, *Nat. Prod. Rep.*, 2024, **41**, 469–511.
6 S. Duquesne, D. Destoumieux-Garzon, S. Zirah, C. Goulard, J. Peduzzi and S. Rebuffat, Two enzymes catalyze the maturation of a lasso peptide in *Escherichia coli*, *Chem. Biol.*, 2007, **14**, 793–803.
7 J. Mukhopadhyay, E. Sineva, J. Knight, R. M. Levy and R. H. Ebright, Antibacterial peptide microcin J25 inhibits transcription by binding within and obstructing the RNA polymerase secondary channel, *Mol. Cell*, 2004, **14**, 739–751.
8 S. Mehmood, V. Corradi, H. G. Choudhury, R. Hussain, P. Becker, D. Axford, S. Zirah, S. Rebuffat, D. P. Tieleman, C. V. Robinson and K. Beis, Structural and functional basis for lipid synergy on the activity of the antibacterial peptide ABC transporter McjD, *J. Biol. Chem.*, 2016, **291**, 21656–21668.
9 W. L. Cheung, S. J. Pan and A. J. Link, Much of the microcin J25 leader peptide is dispensable, *J. Am. Chem. Soc.*, 2010, **132**, 2514–2515.
10 S. J. Pan, J. Rajniak, M. O. Maksimov and A. J. Link, The role of a conserved threonine residue in the leader peptide of lasso peptide precursors, *Chem. Commun.*, 2012, **48**, 1880–1882.
11 O. Pavlova, J. Mukhopadhyay, E. Sineva, R. H. Ebright and K. Severinov, Systematic structure-activity analysis of microcin J25, *J. Biol. Chem.*, 2008, **283**, 25589–25595.
12 R. Ducasse, K. P. Yan, C. Goulard, A. Blond, Y. Li, E. Lescop, E. Guittet, S. Rebuffat and S. Zirah, Sequence determinants governing the topology and biological activity of a lasso peptide, microcin J25, *ChemBioChem*, 2012, **13**, 371–380.
13 F. J. Piscotta, J. M. Tharp, W. R. Liu and A. J. Link, Expanding the chemical diversity of lasso peptide MccJ25 with genetically encoded noncanonical amino acids, *Chem. Commun.*, 2015, **51**, 409–412.
14 K. Schiefelbein, J. Lang, M. Schuster, C. E. Grigglestone, R. Striga, L. Bigler, M. C. Schuman, O. Zerbe, Y. Li and N. Hartrampf, Merging flow synthesis and enzymatic maturation to expand the chemical space of lasso peptides, *J. Am. Chem. Soc.*, 2024, **146**, 17261–17269.
15 H. N. Tan, W. Q. Liu, J. Ho, Y. J. Chen, F. J. Shieh, H. T. Liao, S. P. Wang, J. D. Hegemann, C. Y. Chang and J. Chu, Structure prediction and protein engineering yield new insights into microcin J25 precursor recognition, *ACS Chem. Biol.*, 2024, **19**, 1982–1990.
16 K. J. Rosengren, A. Blond, C. Afonso, J. C. Tabet, S. Rebuffat and D. J. Craik, Structure of thermolysin cleaved microcin

J25: extreme stability of a two-chain antimicrobial peptide devoid of covalent links, *Biochemistry*, 2004, **43**, 4696–4702.
17 N. R. Braffman, F. J. Piscotta, J. Hauver, E. A. Campbell, A. J. Link and S. A. Darst, Structural mechanism of transcription inhibition by lasso peptides microcin J25 and capistruin, *Proc. Natl. Acad. Sci. USA*, 2019, **116**, 1273–1278.
18 P. A. Vincent, A. Bellomio, B. F. de Arcuri, R. N. Farías and R. D. Morero, MccJ25 C-terminal is involved in RNA-polymerase inhibition but not in respiration inhibition, *Biochem. Biophys. Res. Commun.*, 2005, **331**, 549–551.
19 K. P. Yan, Y. Li, S. Zirah, C. Goulard, T. A. Knappe, M. A. Marahiel and S. Rebuffat, Dissecting the maturation steps of the lasso peptide microcin J25 in vitro, *ChemBioChem*, 2012, **13**, 1046–1052.
20 A. L. Ferguson, S. Zhang, I. Dikiy, A. Z. Panagiotopoulos, P. G. Debenedetti and A. James Link, An experimental and computational investigation of spontaneous lasso formation in microcin J25, *Biophys. J.*, 2010, **99**, 3056.
21 G. C. A. da Hora, M. Oh, M. C. Mifflin, L. Digal, A. G. Roberts and J. M. J. Swanson, Lasso peptides: Exploring the folding landscape of nature's smallest interlocked motifs, *J. Am. Chem. Soc.*, 2024, **146**, 4444–4454.
22 S. Yin, X. Mi, S. E. Barrett, D. A. Mitchell and D. Shukla, De novo Folding Mechanisms of Lasso Peptides, *bioRxiv*, 2026, DOI: 10.64898/2026.03.30.715466.
23 B. Ye, W. Tian, B. Wang and J. Liang, CASTpFold: Computed Atlas of Surface Topography of the universe of protein Folds, *Nucleic Acids Res.*, 2024, **52**, W194–W199.
24 S. E. Barrett, S. Yin, P. Jordan, J. K. Brunson, J. Gordon-Nunez, G. Costa Machado da Cruz, C. Rosario, B. K. Okada, K. Anderson, T. A. Pires, R. Wang, D. Shukla, M. J. Burk and D. A. Mitchell, Substrate interactions guide cyclase engineering and lasso peptide diversification, *Nat. Chem. Biol.*, 2025, **21**, 412–419.
25 X. Mi, S. E. Barrett, D. A. Mitchell and D. Shukla, LassoESM a tailored language model for enhanced lasso peptide property prediction, *Nat. Commun.*, 2025, **16**, 8545.
26 X. Ouyang, X. Ran, H. Xu, R. Al-Abssi, Y.-L. Zhao, A. J. Link and Z. J. Yang, LassoPred: a tool to predict the 3D structure of lasso peptides, *Nat. Commun.*, 2025, **16**, 5497.
27 A. Bellomio, P. A. Vincent, B. F. de Arcuri, R. A. Salomon, R. D. Morero and R. N. Farias, The microcin J25 beta-hairpin region is important for antibiotic uptake but not for RNA polymerase and respiration inhibition, *Biochem. Biophys. Res. Commun.*, 2004, **325**, 1454–1458.
28 R. E. de Cristobal, J. O. Solbiati, A. M. Zenoff, P. A. Vincent, R. A. Salomon, J. Yuzenkova, K. Severinov and R. N. Farias, Microcin J25 uptake: His5 of the MccJ25 lariat ring is involved in interaction with the inner membrane MccJ25 transporter protein SbmA, *J. Bacteriol.*, 2006, **188**, 3324–3328.
29 S. B. Socias, K. Severinov and R. A. Salomon, The Ile13 residue of microcin J25 is essential for recognition by the receptor FhuA, but not by the inner membrane transporter SbmA, *FEMS Microbiol. Lett.*, 2009, **301**, 124–129.
30 I. Mathavan, S. Zirah, S. Mehmood, H. G. Choudhury, C. Goulard, Y. Li, C. V. Robinson, S. Rebuffat and K. Beis, Structural basis for hijacking siderophore receptors by antimicrobial lasso peptides, *Nat. Chem. Biol.*, 2014, **10**, 340–342.
31 T. A. Knappe, F. Manzenrieder, C. Mas-Moruno, U. Linne, F. Sasse, H. Kessler, X. Xie and M. A. Marahiel, Introducing lasso peptides as molecular scaffolds for drug design: engineering of an integrin antagonist, *Angew. Chem., Int. Ed.*, 2011, **50**, 8714–8717.
32 J. D. Hegemann, M. De Simone, M. Zimmermann, T. A. Knappe, X. Xie, F. S. Di Leva, L. Marinelli, E. Novellino, S. Zahler, H. Kessler and M. A. Marahiel, Rational improvement of the affinity and selectivity of integrin binding of grafted lasso peptides, *J. Med. Chem.*, 2014, **57**, 5829–5834.
33 A. Lechner, P. A. Jordan, G. C. Machado da Cruz, J. Lamson, J. Gordon, B. K. Okada, K. Anderson, R. Chaudhari, C. J. Rosario, J. Mikesell, S. A. McPhee and M. J. Burk, Overcoming immune checkpoint inhibitor resistance with potent, selective dual avb6/8 inhibitors based on engineered lasso peptides, *J. Am. Chem. Soc.*, 2025, **147**, 32522–32536.
34 D. A. Guarracino, D. V. Carson, T. G. Johnson and A. J. Link, Probing thrombosis initiation with lasso peptide variants as inhibitors to the von Willebrand protein–collagen interaction, *ChemBioChem*, 2025, **26**, e202500188.
35 J. A. Getz, J. J. Rice and P. S. Daugherty, Protease-resistant peptide ligands from a knottin scaffold library, *ACS Chem. Biol.*, 2011, **6**, 837–844.
36 H. Yu, Z. Ma, S. Meng, S. Qiao, X. Zeng, Z. Tong and K. C. Jeong, A novel nanohybrid antimicrobial based on chitosan nanoparticles and antimicrobial peptide microcin J25 with low toxicity, *Carbohydr. Polym.*, 2021, **253**, 117309.
37 H.-T. Yu, J.-Q. Zhang, M.-C. Sun, H. Chen, X.-M. Shi, F.-P. You and S.-Y. Qiao, Polymeric Nanohybrids Engineered by Chitosan Nanoparticles and Antimicrobial Peptides as Novel Antimicrobials in Food Biopreservatives: Risk Assessment and Anti-Foodborne Pathogen Escherichia coli O157:H7 Infection by Immune Regulation, *J. Agric. Food Chem.*, 2022, **70**, 12535–12549.
38 C. Zong, M. O. Maksimov and A. J. Link, Construction of Lasso Peptide Fusion Proteins, *ACS Chem. Biol.*, 2016, **11**, 61–68.